



# Microfluidic production of porous carbon spheres with tunable size and pores



Han Ge<sup>a</sup>, Hongbao Xu<sup>b</sup>, Tianyi Lu<sup>c</sup>, Jiang Li<sup>b</sup>, Haosheng Chen<sup>d</sup>, Jiandi Wan<sup>c,\*</sup>

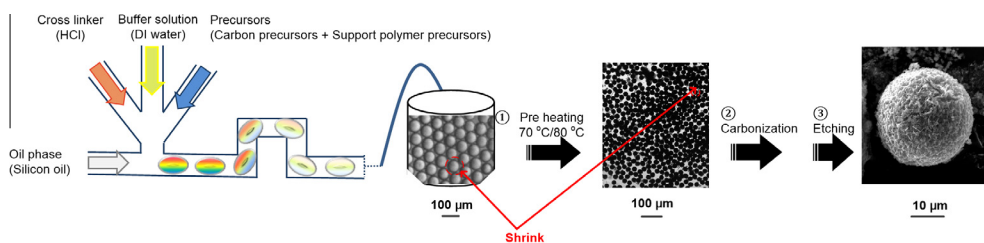
<sup>a</sup>Ocean College, Zhejiang University, Hangzhou 310058, China

<sup>b</sup>School of Mechanical Engineering, University of Science and Technology Beijing, Beijing 100083, China

<sup>c</sup>Microsystems Engineering, Rochester Institute of Technology, NY 14623, USA

<sup>d</sup>State Key Laboratory of Tribology, Tsinghua University, Beijing 100084, China

## GRAPHICAL ABSTRACT



## ARTICLE INFO

### Article history:

Received 27 July 2015

Revised 31 August 2015

Accepted 7 September 2015

Available online 15 September 2015

### Keywords:

Microfluidic

Porous carbon particles

## ABSTRACT

Porous carbon particles have been widely used in many areas including energy storage. Production of carbon microspheres in an efficient, controlled, and low-cost manner, however, is challenging. Here, we demonstrate a microfluidic approach to generate porous carbon particles using inexpensive precursors and show that the size of the particle and pores can be tuned by adjusting the deionized (DI) water content in droplets and preheating temperature. The developed strategy offers an effective approach to control the production of porous carbon spheres with a well-defined diameter, narrow size distribution and pore size.

© 2015 Elsevier Inc. All rights reserved.

## 1. Introduction

Carbon materials, especially porous carbons are of great interest due to their wide range of applications in environment [1], energy [2] and biomedicine [3]. Spherical carbon particles, for examples, have been used for pollutant adsorption [4], water purification [5], and drug delivery [6]. In particular, because of their large surface-volume ratio and high packing capacity, porous carbon microspheres are promising materials for construction of effective electrical energy storage devices such as super capacitors [7].

Indeed, a recently developed electrochemical flow capacitor (EFC) has utilized a flowable carbon microspheres–electrolyte mixture as the active material for capacitive energy storage and shown combined advantages of both super capacitors and flow batteries [8]. For EFC, the composition of the carbon slurry determines the rheological and electrochemical properties of the slurry and thus is critically important for the development of effective EFC. Spherical carbon particles with a narrow size distribution can achieve a smooth flow pattern by minimizing the flow-induced particle segregation and clogging and are highly preferred in EFC.

Conventional approaches used to produce porous spherical carbons such as sol–gel reaction [9], hydrothermal treatment [5], nanocasting [10] and atomizer spray [11], have either harsh reactive conditions or the size of obtained particles are

\* Corresponding author at: Microsystems Engineering, Rochester Institute of Technology, 168 Lomb Memorial Drive, Rochester, NY 14623, USA.

E-mail address: [jdween@rit.edu](mailto:jdween@rit.edu) (J. Wan).

poly-dispersed. Although the size of porous carbon particles generated via the nanocasting method could be mono-dispersed given that the template particles have a uniform size, it becomes time consuming and tedious when change of the size of particles is required [10]. Herein, we develop a microfluidic approach to synthesize porous carbon spheres with a narrow particle size distribution and demonstrate that the size of the carbon particles and pores can be controlled effectively. In particular, we utilize inexpensive and environment-friendly sucrose as the carbon precursor to produce sucrose-containing aqueous droplets via double emulsion (water-in-oil) microfluidics. When the aqueous droplets are solidified at an elevated temperature and carbonized, micrometer diameter spherical carbons are obtained with a much smaller diameter than that of droplets. Most importantly, by changing the deionized (DI) water content of sucrose-containing droplets and preheating temperature, we are able to control the diameter and pore size of obtained carbon particles.

## 2. Methods

### 2.1. Materials and microfluidic methods

The microfluidic chips were fabricated in Polydimethylsiloxane (PDMS) using the soft lithograph method [12], and treated with n-octyltriethoxy silane before using to make the glass surface of the channel hydrophobic. The aqueous phase consists of a precursor solution, DI water and a solution of hydrogen chloride (HCl) (37 wt% in water, Aldrich). The precursor solution is made by dissolving 5 g sucrose in a 5 ml sodium silicate solution (~14% sodium hydroxide (NaOH) and ~27% silicon dioxide (SiO<sub>2</sub>), Aldrich) and 5 ml DI water at 50–80 °C. The reaction takes place when pH < 1, and the molar ratio of sucrose to SiO<sub>2</sub> is kept as 0.65 to ensure the *in-situ* formation of silica networks [13]. Silicon oil with 1 wt% 749 (Dow corning) is used as the continuous oil phase. All the liquids are loaded into four 1 ml syringes and pumped into the microfluidic channel by four syringe pumps (NE 300). The three vertical inlet channels are for the aqueous phases: carbon/silica precursors and HCl solutions are injected from the side channels whereas DI water is introduced from the middle channel and acts as the separating phase. The continuous oil phase is introduced from the lateral channel in which aqueous droplets containing a mixture of carbon/silica precursors, HCl, and DI water are generated. The height of the channels, which is defined as the distance from the glass surface to the top of the PDMS channel, is uniformly 30 μm. The width of the channel, which is defined as the distance between the two opposite PDMS channel walls, for aqueous phase and oil phase is 50 μm and 100 μm, respectively. In our experiment, the flow rate of aqueous phase is adjusted between 0.2 μl min<sup>-1</sup> and 1 μl min<sup>-1</sup>, and the oil phase is adjusted between 1 μl min<sup>-1</sup> and 15 μl min<sup>-1</sup>.

### 2.2. Generation of carbon particles

Sucrose-containing drops are collected into oil with surfactant 749, and heated at 70 °C or 80 °C in a convection oven for 24 h to polymerize the drops and evaporate water. Then, the obtained solid particles are collected on a ceramic crucible after washing out the oil with petroleum ether for more than 5 times. After that, the solid particles will be heated at 200 °C (with a heating rate of 3 °C/min from room temperature) for 12 h under a nitrogen atmosphere. The temperature is then increased to 850 °C with a heating rate of 5 °C/min, and maintained for 3 h. The resulting carbon/silica composites are immersed in a 3 M NaOH solution for 120 h at 70 °C to remove the silica template. The final carbon particles are retrieved by filtration and washed using DI water and ethanol.

Note that the overall yield of the production of porous carbon particles is about 80%. Although the yield of the generation of cured particles from emulsion drops is high (~100%), decreased number of carbon/silica particles during the carbonization process and uncompleted removal of silica from carbon/silica particles lead to a decreased overall yield of porous carbon particles. Comparing to other approaches where the yield of controlled carbonization of sucrose using sulfuric acid is about 50% [14], however, the yield of porous carbon particles in our approaches can be considered high.

### 2.3. Data analysis and SEM imaging

The generation of droplets is observed directly using a high-speed video camera (Phantom M110, 1600 frames per second) mounted on a Leica microscope. The size and size distributions of droplets gathered from the microfluidic channel and polymerized solid particles are analyzed by ImageJ<sup>®</sup>. Also, to check the water evaporation extent of the droplets, the structure of the droplets before and after heating is analyzed by Fourier Transform Infrared Spectroscopy (FTIR) (Bruker). The surface morphology, pores of the particles, and element composition of the particles are analyzed by Scanning Electron Microscopy (SEM) (LYRA3 TESCAN). For each sets of experiments, we have collected data from 3 to 5 pictures, and measured 100 particles and 10 pore size for each particle. The resolution of the images is 300 × 326 pixels per inch (ppi).

Before the SEM analysis, cured particles are washed with petroleum ether for 5–6 times to remove the remained silicon oil. The NaOH etched particles are washed with ethanol and DI water for 5 times before transferred onto the conducted tape. To increase the conductivity of the particles for SEM measurement, the particles are all coated with a layer of Pt.

## 3. Results and discussion

We design and fabricate a variant of the T-junction microfluidics to generate sucrose-containing aqueous droplets in a continuous oil phase. As shown in Fig. 1A, carbon/silica precursors, DI water, and HCl solutions are injected from three independent inlets and form aqueous drops in an oil phase. Here, DI water acts as the buffer to prevent the precursors and HCl reacting before the droplet formation. Immediately after the formation of droplets, they appear as coffee beans with three aqueous reagents stratifying from each other. As the drops go through the serpentine mixing channel, the stratified coffee beans turn to homogeneous white beans, implying that the reagents inside the droplets have mixed well with each other. The whole mixing process is conducted on-chip and completed in tens of milliseconds. The rationale of using on-chip mixing is that the hydrolysis process of the precursor solution is very rapid. Consequently, if HCl and the precursor solution are mixed off-chip, gelation will occur rapidly, resulting in a high viscous solution. Formation of emulsion drops using such solution as the disperse phase will be extremely difficult. In addition, mixing of HCl, DI water, and the precursor solution “on-chip” can provide an *in-situ* capability to tune the ratio between the reactants, which is not accessible to other non-microfluidic approaches or bulk reactions.

The obtained drops are then collected and heated at 70 °C or 80 °C to produce solid particles. Fig. 1A-I and A-II are images of collected drops and solidified particles after heating, respectively. Fig. 1A-III shows the polydispersity of the particles. The polydispersity index (PDI) calculated based on the expression of  $PDI = (D_{max} - D_{min})/D_{avg}$  where  $D_{max}$  is the maximum diameter of the statistic particles,  $D_{min}$  is the minimum diameter of the statistic particles, and  $D_{avg}$  is the average diameter of the particles, is about

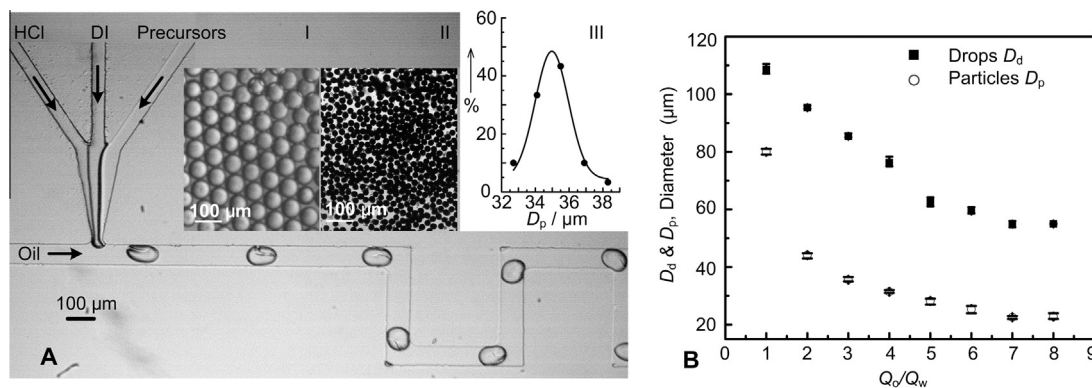


**Fig. 1.** Microfluidic production of droplets and particles. (A) Image of the generation of carbon precursor-containing drops in microfluidics. (I) and (II) are the images of droplets before and after preheating at 80 °C, respectively. (III) Size distribution of the obtained particles in (II). Polydispersity index (PDI) = 0.157. (B) Dependence of the diameter of drops ( $D_d$ ) and preheating-obtained particles ( $D_p$ ) on the oil-to-water flow rate ratio ( $Q_o/Q_w$ ).

0.16, indicating a relatively narrow size distribution. Notably, the diameter of solidified particles ( $D_p$ ) is much smaller than that of drops ( $D_d$ ). In fact, it occurs to all drops generated at different oil-to-water flow rate ratios ( $Q_o/Q_w$ ) (Fig. 1B). The shrink ratio ( $D_d/D_p$ ) of drops generated at various  $Q_o/Q_w$ , however, remains almost invariant, i.e.,  $D_d/D_p \approx 2.4$  when the flow rates of all aqueous phases including HCl, DI water, and precursor solutions ( $Q_w = Q_{DI+HCl+precursors}$ ) are kept constant. The water content, on the other hand, decreases significantly after heating based on the disappearance of OH absorption band in an FTIR measurement (Fig. S1), suggesting that the size shrink after heating results from the water loss via evaporation.

Accordingly, tuning the water content inside drops can likely control the shrink ratio, and thus produce small carbon particles from relatively large aqueous drops. Indeed, when the DI water content,  $R$ , which is defined as  $Q_{DI}/Q_w$ , is increased, particles with smaller sizes are obtained (Fig. 2A). As  $R$  increases from 0.33 to 0.71, for example,  $D_d/D_p$  increases from 1.3 to 4.2. As a result, 20  $\mu\text{m}$  diameter particles can be obtained from drops with a

diameter of 110  $\mu\text{m}$ . In the experiment,  $Q_o/Q_w$  is kept constant as 5, and the flow rates of other two aqueous phases, i.e., precursors and HCl are also kept constant  $0.2 \mu\text{l min}^{-1}$ , whereas  $Q_{DI}$  is increased to increase the water content of the droplet.  $D_d$  is thus constant due to the constant  $Q_o/Q_w$ , but  $D_p$  is decreased when  $R$  is increased. In addition, we find that particles synthesized from drops with a low DI water content, i.e.,  $R = 0.43$ , have a black color (Fig. S2A) whereas particles synthesized from drops with a high DI water content, i.e.,  $R = 0.71$ , exhibit a dark brown color or even are transparent (Fig. S2B). The observation of different colors of the particles is probably due to the different densification of the solid structure [15]. Indeed, when  $R$  increases up to 0.8, irregular particles start to form (Fig. S3), implying that the solid content inside the particle is too low to support the particle to be a spherical shape. Nevertheless, when the solid particles are carbonized, they can all be converted to carbon particles without notable size change (Fig. 2B and Fig. S4). It should be noted that for a specific value of  $R$ , different flow rates of DI water, HCl solution, and precursor solution have been used. Oil flow rate also

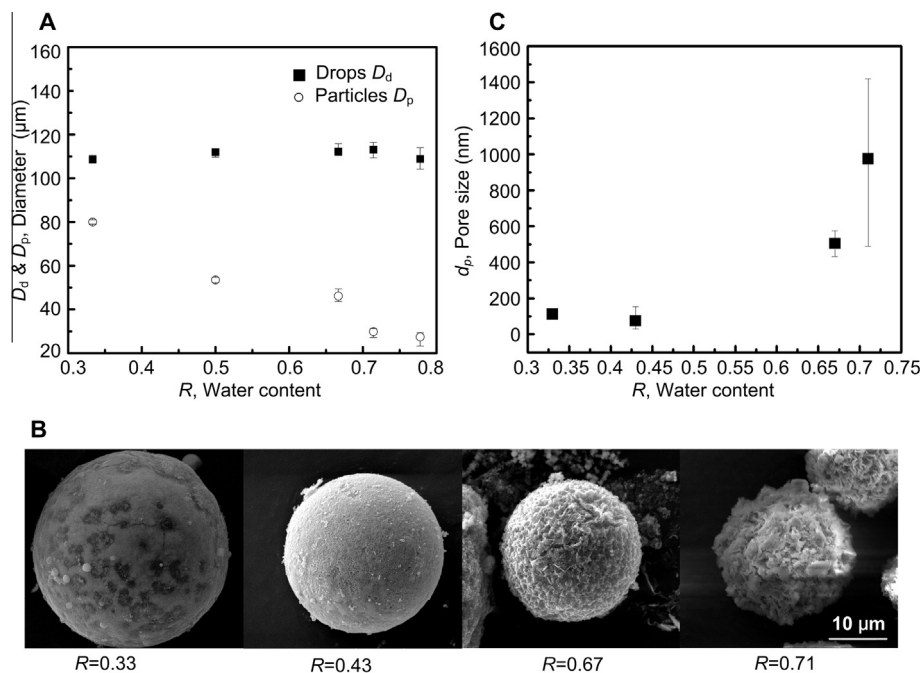


**Fig. 2.** Effects of DI water content ( $R$ ) of drops on the post-synthesized particles' structure. (A) Dependence of the diameter of drops ( $D_d$ ) and preheating-obtained particles ( $D_p$ ) on the DI water content ( $R$ ) of drops. (B) SEM images of carbonized particles obtained from drops with an increased DI water content ( $R$ ). (C) Dependence of the pore size ( $d_p$ ) of carbonized particles on the DI water content ( $R$ ) of drops.

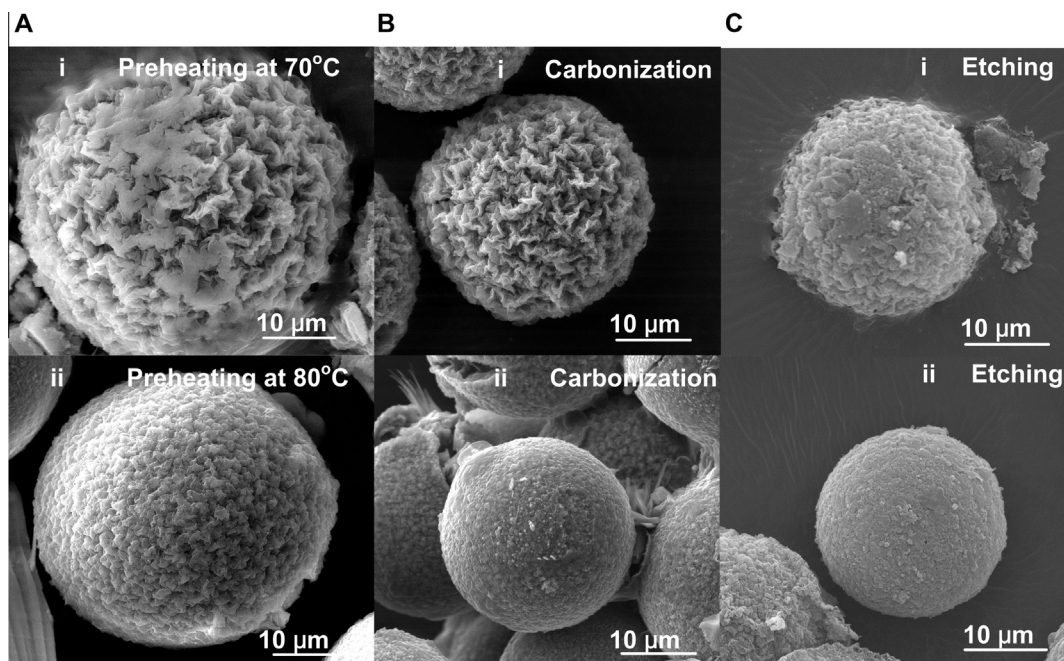


**Fig. 3.** Effects of preheating temperature on the morphology and size of the particles. SEM images of carbon precursor-containing drops (A) after pre-heating at (i) 70 °C and (ii) 80 °C, (B) after carbonization and (C) after NaOH etching.  $R = 0.43$  for the all experiments.

changes accordingly to maintain a constant  $Q_o/Q_w$  ratio in the experiments.

Moreover, the pore size of carbon particles can also be controlled by adjusting the DI water content in drops. As shown in Fig. 2C, after the carbon particles are etched by NaOH, the diameter of the pores ( $d_p$ ) on the surface of the carbon particles increases with the increase of  $R$ . When the DI water content is lower ( $R < 0.45$ ), for example,  $d_p$  is about 100 nm. As  $R$  increases,  $d_p$  reaches as high as 970 nm when  $R$  is 0.71. The dependence of pore size on  $R$  can be explained by the decrease of  $H^+$  concentration inside the droplet [16]. During the sol–gel reaction of silica precursors, the gelation time of the formed silica gel depends strongly on the concentration of acid catalyst [17]. With the increase of  $R$  inside each droplet, the  $H^+$  concentration decreases. As a result, silica clusters aggregate slowly, forming a loose three-dimensional silica network. After the particles are carbonized and the silica network is removed by etching the particles with NaOH, large pores form in the carbon spheres.

Last, we show that the preheating temperature affects the structure of carbon particles. For example, carbon particles synthesized from drops that are preheated at 70 °C and 80 °C have a different morphology and size. Fig. 3 shows the SEM images of the particles obtained from the droplets after preheating at 70 °C and 80 °C (Fig. 3A), and then carbonized (Fig. 3B) and etched by NaOH (Fig. 3C). High heating temperature, i.e., 80 °C, results in a smooth surface and small size whereas the one heated at 70 °C looks like an acanthosphere, with accented wrinkles on its surface. The size reduction may probably due to the thorough water evaporation at high heating temperature. In addition, at high preheating temperature, the rate of crosslinking reaction of silica network increases [18], resulting in a more rigid and dense gel network, which may explain the different morphology between particles heated at 70 °C and 80 °C.

#### 4. Conclusion

We have demonstrated a microfluidic approach to synthesize mono-dispersed porous carbon particles with economical and

environment-friendly precursors. Besides the traditional microfluidic control of the size of the particle by adjusting flow rates [19], we can control the size and pores of the carbon particle by simply changing the DI water content of the droplet before curing. Moreover, we also show that the size and morphology of the synthesized particle can be tuned by changing the preheating temperature. We believe the strategy developed here will provide useful guidelines for high efficiency and low cost fabrication of carbon spheres, which could be used in a wide range of energy storage devices including EFC.

#### Acknowledgments

This work is supported by Foundation of Zhejiang Educational Committee (No. N20110201), Zhejiang Provincial Natural Science Foundation of China (No. LQ13E050001) and NSFC (No. 51405432). J. Wan, T. Lu and H. Ge acknowledge the support from the Kate Gleason College of Engineering at RIT and Donors of the American Chemical Society Petroleum Research Fund for partial support of this research.

#### Appendix A. Supplementary material

Supplementary data associated with this article can be found, in the online version, at <http://dx.doi.org/10.1016/j.jcis.2015.09.018>.

#### References

- [1] K. Sears, L. Dumée, J. Schütz, M. She, H. Chi, S. Hawkins, M. Duke, S. Gray, Recent developments in carbon nanotube membranes for water purification and gas separation, *Materials* 3 (2010) 127–149.
- [2] G.L. Che, B.B. Lakshmi, E.R. Fisher, C.R. Martin, Carbon nanotube membranes for electrochemical energy storage and production, *Nature* 393 (1998) 346–349.
- [3] M. Zheng, A. Jagota, E.D. Semke, B.A. Diner, R.S. Mclean, S.R. Lustig, R.E. Richardson, N.G. Tassi, DNA-assisted dispersion and separation of carbon nanotubes, *Nat. Mater.* 2 (2003) 338–342.
- [4] C.Y. Yin, Y.J. Wei, F.W. Wang, Y.H. Chen, X. Bao, Magnetic hierarchical porous carbon sphere prepared for removal of organic pollutants in water, *Mater. Lett.* 104 (2013) 64–67.

- [5] X.B. Wang, J. Liu, W.Z. Xu, One-step hydrothermal preparation of amino-functionalized carbon spheres at low temperature and their enhanced adsorption performance towards Cr (VI) for water purification, *Colloids Surf. A* 415 (2012) 288–294.
- [6] Y. Fang, D. Gu, Y. Zou, Z.X. Wu, F.Y. Li, R.C. Che, Y.H. Deng, B. Tu, D.Y. Zhao, A low-concentration hydrothermal synthesis of biocompatible ordered mesoporous carbon nanospheres with tunable and uniform size, *Angew. Chem., Int. Ed.* 49 (2010) 7987–7991.
- [7] F.W. Ma, H. Zhao, L.P. Sun, Q. Li, L.H. Huo, T. Xia, S. Gao, G.S. Pang, Z. Shi, S.H. Feng, A facile route for nitrogen-doped hollow graphitic carbon spheres with superior performance in supercapacitors, *J. Mater. Chem.* 22 (2012) 13464–13468.
- [8] V. Presser, C.R. Dennison, J. Campos, K.W. Knehr, E.C. Kumbur, Y. Gogotsi, The electrochemical flow capacitor: a new concept for rapid energy storage and recovery, *Adv. Energy Mater.* 2 (2012) 895–902.
- [9] S. Gangolli, R.E. Partch, E. Matijevic, Preparation of highly porous spherical colloidal carbon particles, *Colloids Surf.* 41 (1989) 339–344.
- [10] D.C. Wu, Y.R. Liang, X.Q. Yang, Z.H. Li, C. Zou, X.H. Zeng, G.F. Lv, R.W. Fu, Direct fabrication of bimodal mesoporous carbon by nanocasting, *Micropor. Mesopor. Mater.* 116 (2008) 91–94.
- [11] J.E. Hampsey, Q.Y. Hu, L. Rice, J.B. Pang, Z.W. Wu, Y.F. Lu, A general approach towards hierarchical porous carbon particles, *Chem. Commun.* 28 (2005) 3606–3608.
- [12] J.R. Anderson, D.T. Chiu, F.J. Jackman, O. Cherniavskaya, J.C. McDonald, H.K. Wu, S.H. Whitesides, G.M. Whitesides, Fabrication of topologically complex three-dimensional microfluidic systems in PDMS by rapid prototyping, *Anal. Chem.* 72 (2000) 3158–3164.
- [13] S.J. Han, M. Kim, T. Hyeon, Direct fabrication of mesoporous carbons using in-situ polymerized silica gel networks as a template, *Carbon* 41 (2003) 1525–1532.
- [14] J.C. Zhang, W.Q. Shen, D.Y. Pan, Z.W. Zhang, Y.Q. Fang, M.H. Wu, Controlled synthesis of green and blue luminescent carbon nanoparticles with high yield by the carbonization sucrose, *New J. Chem.* 34 (2010) 591–593.
- [15] R.J.D. Tilley, *Understanding Solids: The Science of Materials*, second ed., John Wiley & Sons, West Sussex, U.K., 2013, pp. 445–489.
- [16] J.L. Gurav, A.V. Rao, A.P. Rao, D.Y. Nadargi, S.D. Bhagat, Physical properties of sodium silicate based silica aerogels prepared by single step sol-gel process dried at ambient pressure, *J. Alloys Compd.* 476 (2009) 397–402.
- [17] P.B. Sarawade, J.K. Kim, A. Hilonga, D.V. Quang, H.T. Kim, Synthesis of hydrophilic and hydrophobic xerogels with superior properties using sodium silicate, *Micropor. Mesopor. Mater.* 139 (2011) 138–147.
- [18] R. Takahashi, K. Nakanishi, N. Soga, Effects of aging and solvent exchange on pore structure of silica gels with interconnected macropores, *J. Non-Cryst. Solids* 189 (1995) 66–76.
- [19] S.Q. Xu, Z.H. Nie, M. Seo, P. Lewis, E. Kumacheva, H.A. Stone, P. Garstecki, D.B. Weibel, I. Gitlin, G.M. Whitesides, Generation of monodisperse particles by using microfluidics: control over size, shape, and composition, *Angew. Chem.* 117 (2005) 734–738.